



# Nondestructive silicon wafer recovery by a novel method of solvothermal swelling coupled with thermal decomposition

Xinhai Xu<sup>a,b</sup>, Dengguo Lai<sup>a,\*</sup>, Gang Wang<sup>a,b</sup>, Yin Wang<sup>a,\*</sup>

<sup>a</sup> CAS Key Laboratory of Urban Pollutant Conversion, Institute of Urban Environment, Chinese Academy of Sciences, Xiamen 361021, China

<sup>b</sup> University of Chinese Academy of Sciences, Beijing 100049, China

## ARTICLE INFO

### Keywords:

Photovoltaic module  
Waste treatment  
Gas release channel  
Intact silicon wafer  
Resource recovery

## ABSTRACT

End-of-life (EoL) photovoltaic (PV) waste is becoming a severe environmental issue worldwide. Developing technologies to reclaim nondestructive and reusable silicon wafers (Si-wafers) is the most appealing way to solve this problem, saving ~40% on PV module production costs, but it remains a great challenge. Herein, we develop a novel method of coupling solvothermal swelling with thermal decomposition (SSTD) for structure-intact Si-wafers recovery. Laboratory-scale studies reveal that undamaged Si-wafers can be easily obtained by conducting a solvothermal swelling process in advance to build channels for the quick, horizontal release of ethylene-vinyl acetate (EVA) thermal decomposition gas. Using scaling-up equipment, 86.11% of Si-wafers in commercial PV module are reclaimed without any damage, nearly 10-fold higher than that of thermal decomposition alone (9.26%). Moreover, PV backsheets can be depolymerized with specially designed solvents (toluene-ethanol), greatly facilitating swelling by exposing EVA directly to toluene vapor and reducing the emission of fluorine-containing gas pollutants. The reclaimed Si-wafers are comparable to the originals, with the following properties: interstitial oxygen,  $<6 \times 10^{17}$  atoms-cm<sup>-3</sup>; substitutional carbon,  $<5 \times 10^{17}$  atoms-cm<sup>-3</sup>; resistivity, 1.84 Ω-cm; and minority carrier lifetime, 3.92 μs.

## 1. Introduction

The fast-growing development of environmentally friendly energy generation methods have brought about the explosion of photovoltaic (PV) modules in recent decades. To date, the estimated global cumulative installed capacity of PV modules has dramatically increased from 40 GW in 2010 to 715 GW in 2020 [1]. In this regard, the limited lifetime (~25 years) of PV modules will lead to a significant amount of EoL PV modules, which has been defined as a new waste of electrical and electronic equipment [2], becoming a severe challenge to the sustainable energy generation system and an increasingly serious environmental issue [3–9]. Thus, it is necessary to develop novel technologies for PV modules waste disposal, particularly for crystalline silicon (c-Si) solar panels, which dominate 85–90% market share [10].

Currently, improper landfilling of PV module wastes is intolerable due to the leaching of hazardous heavy metals (e.g., lead and cadmium) [7,9]. Instead, collection and recycling is becoming the general trend. The high-value Si-wafers reuse and metals recovery from EoL PV module are significantly important to reduce their potential environmental risks and the production cost, supporting the sustainable development of PV

industry [11–14]. Generally, the c-Si PV module has a sandwich-like structure, in which the cells are bonded with the upper tempered glass and backsheets by EVA adhesive material. Therefore, some approaches have been developed to first remove EVA to separate these layers and then recycle valuable resources in recent years. Bruton et al. used nitric acid (HNO<sub>3</sub>) to remove EVA, but this process is always accompanied by high acid consumption and harmful NO<sub>x</sub> emissions [15]. In addition, EVA removal by immersing PV modules in organic solvents has been reported; however, this method always consumes large amounts of organic solvents and takes a long time over several weeks [16]. Moreover, these methods are proven to be insufficient for complete EVA removal [17]. Thermal decomposition or burning at 480–600 °C is considered to be able to remove EVA completely but brings a new problem of harmful gas release because the backsheets contain fluorinated compounds [18–20]. Thus, assisted processes, such as thermal pretreatment at 200 °C or mechanical pretreatment, are selected to remove the backsheets beforehand [21–23]. Despite all these efforts, unbroken Si-wafer is rarely reclaimed. Furthermore, it appears increasingly difficult to recover nondestructive Si-wafer since the thickness was reduced to less than 200 μm after 2006 [24,25]. To date,

\* Corresponding authors.

E-mail addresses: [dglai@iue.ac.cn](mailto:dglai@iue.ac.cn) (D. Lai), [yinwang@iue.ac.cn](mailto:yinwang@iue.ac.cn) (Y. Wang).

<https://doi.org/10.1016/j.cej.2021.129457>

Received 7 January 2021; Received in revised form 10 March 2021; Accepted 17 March 2021

Available online 24 March 2021

1385-8947/© 2021 Elsevier B.V. All rights reserved.

reclaimed fragmented Si-wafers can only be used as raw materials for silicon ingots production, which causes much energy consumption and hazardous gases emission [26].

In fact, one of the important reasons responsible for the power degradation of PV modules is the decomposition or aging of EVA, while the lifetime of Si-wafers is much longer than that of modules [16]. In this case, if structurally intact Si-wafers are reclaimed to be directly reused in the new PV module fabrication, the silicon ingot reproduction and wafer manufacturing process can be omitted. Such an ideal recycling mode, therefore, can avoid the high energy consumption and environment pollution, as well as reduce approximately 40% cost of PV module production [27]. Unfortunately, only a few methods have been reported to recycle nondestructive Si-wafer, such as using a thermal process with a fixture of PV modules at a specific heating rate ( $15\text{ }^{\circ}\text{C}\cdot\text{min}^{-1}$ ) [28] and a method breaking the tempered glass before thermal decomposition [29]. Although they offer the probability for nondestructive Si-wafer recovery, the complicated EVA thermal decomposition process is actually difficult to control and glass cracking tends to break Si-cell at the same time. Those processes are still unstable and uncontrollable, making practical applications difficult. Therefore, developing easily scaled-up and controllable nondestructive Si-wafer reclaiming technology is urgent and still a great challenge.

In this study, for the first time, a feasible, facile and controllable method integrating solvothermal swelling and thermal decomposition for nondestructive Si-wafer recovery is developed. The trapped EVA thermal decomposition gas between Si-cells and glass are found to be the main factor leading to the breakage of Si-wafers. Under the optimized operating parameters of solvothermal swelling, including treatment temperature, processing duration and organic solvents quantity, channels for trapped gas release can form in a short time, and therefore, nondestructive Si-wafers are easily obtained after thermal decomposition. As a result, an integrity rate nearly 10-fold higher than that of thermal decomposition alone is achieved. Additionally, solvothermal swelling provides significant time and organic solvent savings, and the PV backsheet removal, exhibiting low environmental pollution feature. Furthermore, the process mechanism is investigated, and the characteristics of reclaimed Si-wafers are tested to prove the feasibility of their reuse for new PV module fabrication. From a laboratory-scale to scaled up device, the proposed SSTD process is demonstrated as a stable and controllable method for massive nondestructive and reusable Si-wafer reclamation.

## 2. Materials and methods

### 2.1. Materials

A mini PV module containing one multicrystalline silicon (mc-Si) solar cell ( $39\text{ mm} \times 19\text{ mm} \times 220\text{ }\mu\text{m}$ ) was used for parameter optimization. The mini-module composed of low-iron tempered glass ( $50\text{ mm} \times 50\text{ mm} \times 3.2\text{ mm}$ ), EVA ( $400\text{ }\mu\text{m}$ -thick), TPT (Tedlar/PET (polyethylene terephthalate)/Tedlar) backsheet ( $300\text{ }\mu\text{m}$ -thick) and mc-Si solar cell was laminated at  $150\text{ }^{\circ}\text{C}$  for 12 min. In addition, commercial solar panels ( $230\text{ mm} \times 240\text{ mm}$ , HT-P5W-36P, Hetech Energy) contained 36 mc-Si cells ( $52\text{ mm} \times 19\text{ mm} \times 220\text{ }\mu\text{m}$ ) were used for the scale-up experiment to verify the optimized parameters. The reagents used in this work were purchased from the Sinopharm Chemical Reagent Co., Ltd.

### 2.2. Experimental procedure

The mini-module was pretreated in a solvothermal reactor with a volume of 200 mL (KH-200 mL, Mogina Instrument Manufacturing Co., Ltd.), where the organic solvents were added. The reactor was heated to form hot organic solvent vapor to swell the EVA and build gas release channels. The pretreated module was placed in a furnace (QSH-1700 W, Shalarge Furnace Co., Ltd.) for complete decomposition/combustion of

the residual EVA and backsheet in an air ambient. For scale-up demonstration, an enlarged solvothermal reactor with a volume of 25 L (CF-25L, Global Chemical Machinery MFG Co., Ltd.) was utilized to recycle Si-wafers from commercial solar panels. Finally, to evaluate the reuse feasibility of reclaimed wafers, the impurities on reclaimed cells were removed by chemical etching.

### 2.3. Analysis and characterization

To quantitatively determine the integrity rate of the reclaimed Si-wafer, the area of each piece of reclaimed wafer was measured by Image J software. The integrity rate of reclaimed Si-wafers from mini-modules (Eq. (1)) and commercial modules (Eq. (2)) is defined as follows:

$$i = \frac{S_{\max}}{S} \times 100\% \quad (1)$$

where  $i$  is the integrity rate of reclaimed Si-wafers from mini-modules;  $S_{\max}$  is the area of the largest piece from damaged Si-wafers; and  $S$  is the area of unbroken wafers.

$$I = \frac{n}{N} \times 100\% \quad (2)$$

where  $I$  is the integrity rate of Si-wafer recovery from commercial modules;  $n$  is the number of unbroken Si-wafers reclaimed from commercial modules; and  $N$  is the number of Si-cells contained in commercial modules, which is 36.

The weight loss behavior of EVA and backsheet was measured by thermogravimetric analysis (TG 209 F3, NETZSCH, Germany). The variation of major chemical components in organic solvents was analyzed by gas chromatography-mass spectrometry (GC-MS, Shimadzu QP2010Ultra, Japan) to support the process mechanism. The surface morphology and purity analysis of Si-wafers were evaluated by scanning electron microscopy (SEM) equipped with energy dispersive spectrometry (EDS) (S-4800, HITACHI, Japan) and X-ray photoelectron spectroscopy (XPS, ESCALAB 250Xi, Thermo Fisher, USA). The resistivity of wafers was measured by four-point probes (FT-8100, ROOKO). The minority carrier lifetime of reclaimed wafers was evaluated by microwave-based detection of the photoconductivity decay ( $\mu$ -PCD, WT-1000B, Semilab). The concentration of carbon (C) and oxygen (O) in Si-wafers was measured by time-of-flight secondary ion mass spectrometry (TOF-SIMS, IONTOF5, Germany).

## 3. Results and discussion

Here, the cause of Si-wafer breakage is explained. Gas generation during EVA thermal decomposition is found to be the main factor leading to the breakage, which is also confirmed by previous studies [28,29]. According to the structure of the c-Si PV module in Fig. 1a, Si-cells are packaged by two layers of EVA between glass and backsheet. Thus, the gas produced during EVA thermal decomposition in PV module can be divided into two parts. For the EVA layer between cells and backsheet, the produced gas can easily escape thanks to the decomposition of the backsheet at the same time, whose main chain decomposition temperature ( $\sim 415\text{ }^{\circ}\text{C}$ ) is similar to that of EVA ( $\sim 430\text{ }^{\circ}\text{C}$ ), as depicted in Fig. S1 (Supporting Information). For the gas produced from EVA decomposition between cells and glass, there are no channels for them to escape due to the thermal stability of glass. In this case, the generated gas would form closed bubbles between cells and glass, and the gas accumulation and inner gas pressure in bubbles would constantly increase as the temperature increases and EVA decomposition occurs. Due to the much higher strength of glass than that of Si-cells, the accumulated gas tends to escape by penetrating Si-cells once the bubbles expanding force is higher than the critical strength of the cells, thereby leading to the breakage. In this regard, the major obstacle to

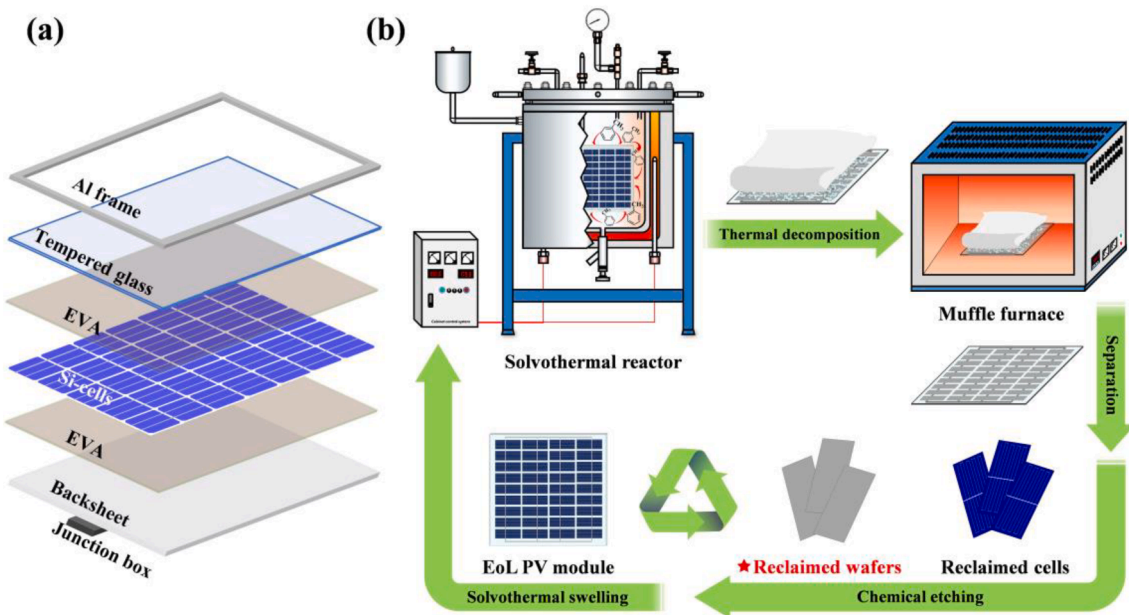


Fig. 1. Schematic diagram of the (a) c-Si PV module structure and (b) Si-wafer nondestructive recovery system with solvothermal swelling-thermal decomposition technology.

nondestructive Si-wafer reclamation mainly arises from the lack of gas-releasing channels.

To recycle structurally intact wafers, a novel method by coupling solvothermal swelling with thermal decomposition was developed. The schematic diagram of Si-wafer nondestructive recovery system using SSTD technology is shown in Fig. 1b. In the system, PV modules were pretreated by exposing to hot and pressurized organic vapors to achieve EVA swelling and build gas release channels. It should be noted that toluene, a nonhazardous solvent [30], has been proven to be effective for EVA dissolution [17], therefore, toluene was directly selected as the solvent here. Compared to the conventional method of immersing PV modules in organic solvents [16], solvothermal swelling provides significant time and organic solvent savings. In addition, the milder condition enables solvothermal swelling with higher superiority and controllability in recycling structure-intact Si-wafers over other methods, of which immersion is assisted with ultrasonic or heating to speed up EVA dissolution [17,31]. Afterwards, the pretreated modules were placed in a furnace for the complete removal of residual EVA and

backsheet at 500 °C, according to the thermogravimetric analysis (Fig. S1). During the thermal combustion process, the EVA decomposition gas escape horizontally through the formed release channels instead of vertically penetrating Si-cells. This being so, the solvothermal swelling plays a decisive role in the SSTD process, and its operating parameters were first studied under the same thermal decomposition condition of 500 °C, and the detailed operating conditions are shown in Table S1.

### 3.1. Parameter optimization of solvothermal swelling

The solvothermal temperature, processing duration and quantity of organic solvents for nondestructive Si-wafer recovery were optimized using mini-modules with a single Si-wafer, and the results are depicted in Fig. 2. The effect of the solvothermal temperature on the integrity rate (i) of Si-wafers was investigated over a range of 120–210 °C and under the conditions of an excessive processing duration of 4 h and 0.5 M toluene. Compared to the control group (Si-wafers reclaimed by thermal

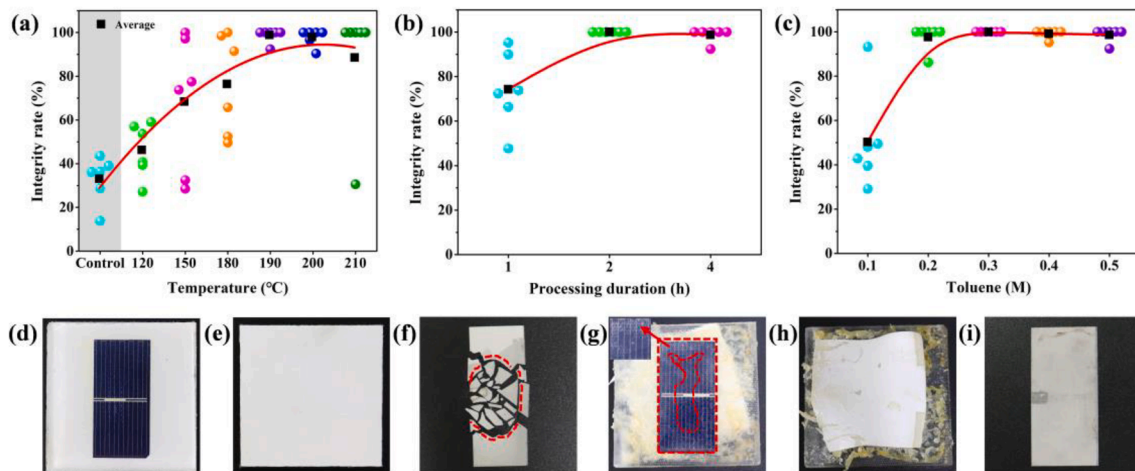


Fig. 2. Integrity rate variation with different (a) solvothermal temperatures, (b) processing duration and (c) quantities of toluene. Optical photos of the (d) front and (e) back of the initial module, (f) cell reclaimed by thermal treatment only, (g) front and (h) back of the module after solvothermal swelling, and (i) cell reclaimed by SSTD technology.

decomposition alone) with an average integrity rate of 32.93%, Si-wafers reclaimed by SSTD technology exhibit a much higher average integrity rate of up to 98.72%, and the integrity rate increases with increasing treatment temperature. When the temperature reaches 190 °C, unbroken Si-wafers are stably obtained. However, a higher temperature over 210 °C may raise the risk of cracking Si-cells in solvothermal swelling process. Accordingly, a temperature of 190 °C was selected to optimize the processing duration. As presented in Fig. 2b, processing duration of 2 h is sufficient for solvothermal swelling and gas release channels building, and Si-wafers without any damage are obtained. Furthermore, the lower limit quantity of toluene was determined under the condition of the above optimized solvothermal temperature (190 °C) and processing duration (2 h). This shows that most of the wafers would not be damaged until the quantity of toluene dropped to 0.1 M.

The results may reveal that the main factors on EVA swelling are treatment temperature and organic solvent quantity, determining the pressure in reactor and the toluene concentration. The pressure is considered as the swelling driving force, while the toluene concentration directly affects the EVA swelling. With a constant and excessive toluene concentration, the pressure is synonymous with saturated vapor pressure of toluene, determining by Antoine equation (Eq. (3)), where  $P_1$  is the saturated vapor pressure,  $t$  is the temperature and  $A$  (6.95464),  $B$  (1341.8) and  $C$  (219.482) are constant. It indicated that a higher temperature brings a higher driving force, facilitating EVA swelling and the gas-releasing channels formation. Nonetheless, extremely high temperature would make EVA swelling too severe so that the cells breakage. With the constant temperature (190 °C), organic solvent quantity may affect both pressure and toluene concentration. The pressure when toluene concentration below 0.165 M (theoretical,  $P_1 = P_2$ ) is calculated by Eq. (4), where  $P_2$  refers to the pressure,  $n$  refers to the toluene molar,  $R$  (8.314 J/(mol·K)) is constant,  $T$  refers to the temperature and  $V$  (200 mL) refers to the volume of the reactor. In the case of 0.1 M toluene, the pressure (theoretical value of 401.57 kPa) is much lower than that of excessive toluene (theoretical value of 633.39 kPa) and the residual solvent after solvothermal swelling process is observed. Therefore, it may be suggested that unsuccessful recovery of nondestructive Si-wafers under lower organic solvent quantity is also attributed to an insufficient swelling driving force.

$$\lg P_1 = A - \frac{B}{t + C} \quad (3)$$

$$P_2 = \frac{nRT}{V} \quad (4)$$

Fig. 2d–i intuitively present the appearance of mini-modules before and after sequence treatment. Fig. 2d and e are the front and back photos of the initial mini-module, respectively. By thermal decomposition alone, fragmented Si-cells were obtained and the damage area distributed as an elliptical shape, as depicted in Fig. 2f. In addition, many gas bubbles between glass and Si-cells and round or elliptical damage area of broken Si-cells in commercial PV module can be observed after thermal treatment alone at 300 and 500 °C, respectively (Fig. S2). Of course, not all damage areas appear round or elliptical shape because the gas pressure is complex during thermal treatment. The results above may support the speculation that gas due to EVA decomposition form bubbles and are trapped between glass and Si-cells, which contributed to the Si-cells damage once the pressure exceeds the strength of Si-cells. Accordingly, a foregoing solvothermal swelling treatment is integrated to build decomposition gas release channels. Visually, as shown in Fig. 2h, part of the EVA is removed, and the residual EVA becomes loose, folded and non-adhesive after solvothermal swelling under optimized parameters (190 °C, 2 h, 0.2 M toluene). From the front side in Fig. 2g, many macroscopic bubbles filled with liquefied organic solvent formed between Si-cells and glass, permeating gradually from the cell edge to the center. This suggests that EVA decomposition gas can escape against

the solvent permeation route. In other words, gas release channels are successfully built via solvothermal swelling. As a result, coupled with thermal decomposition treatment, nondestructive recycling of Si-cell from the module is achieved (Fig. 2i).

A notable phenomenon can be observed that the backsheets do not show any breakage or significant change except shape curling during the swelling of EVA, which is undesired. The covered backsheets hinder the direct interaction of EVA and toluene, which makes the EVA swelling inefficient at the beginning and increases the difficulty of the process. This means more toluene and higher temperature to generate higher pressure driving force, and prolonged processing duration are necessary. Hence, the removal of backsheets would be of great significance. To achieve this, we provide a specially designed mixed organic solvents system, in which a small amount of ethanol is introduced into the solvothermal swelling process. Ethanol introduction is expected to achieve backsheets removal, and the mechanism will be discussed in the next section. Importantly, ethanol can also react as a good solvent to provide an additional pressure driving force as a replacement for a portion of toluene. In short, ethanol participation is able to improve the utilization efficiency of toluene and make the recovery system more environmentally friendly.

The effect of the ethanol molarity on the integrity rate of Si-wafers was investigated at 190 °C for 2 h with 0.1 M toluene. Note that this condition has been proven unavailable for nondestructive Si-wafer reclamation before due to insufficient toluene, as shown in Fig. 2c. In Fig. 3a, the integrity rate of Si-wafers increases after ethanol addition, and backsheets depolymerization into pieces and even powders can be observed (Fig. 3c–e). The highest average integrity rate of 84.02% is achieved by adding 0.2 M ethanol, which is an increase of by 66.81% compared to the original case without adding ethanol (50.37%). This implies that ethanol addition facilitates the swelling process due to the backsheets removal, exposing EVA to toluene vapor directly and enhancing the driving force derived from ethanol vapor. However, a continuously increased ethanol molarity is not allowed because the integrity rate of Si-wafers significantly decreases from 84.02% to 61.08% when the ethanol molarity increases from 0.2 M to 0.6 M. Increased ethanol addition would induce more severe TPT depolymerization, along with a more vigorous swelling reaction, which may lead to the uncontrollable process and cause undesired Si-wafer breakage. More importantly, excessive ethanol would corrode the aluminum electrode due to the release of protons at the subcritical state for ethanol (190 °C). In this case, the protons react with aluminum and remove the aluminum electrode layer, as presented in Fig. 3h. The reduced thickness of the aluminum electrode is approximately 20 μm, which would decrease the mechanical strength and pressure resistance capability of Si-cells, thereby reducing the integrity rate of reclaimed Si-wafers. In addition, toluene is proven to be indispensable since no unbroken wafer can be obtained when toluene is absent, with an average integrity rate of 46.55%. As depicted in Fig. 3e, despite the backsheets removal, EVA still maintains a dense structure and high toughness without any gas-releasing channels, inhibiting the gas escape and leading to breakage. This is also evidence that the backsheets have a negligible effect on the thermal decomposition process for unbroken wafer recovery. EVA decomposition gas generated between cells and glass are the main cause of cell breakage, as pointed out before, rather than between cells and backsheets.

### 3.2. Verification in a scale-up facility

To verify the feasibility of the proposed SSTD process, nondestructive Si-wafer recovery from commercial modules was investigated using a scale-up facility. The temperature of 190 °C, processing duration of 2 h, 0.2 M toluene and 0.2 M ethanol were adopted, and the integrity rate ( $I$ ) of the wafers was calculated. As a comparison, the Si-wafers reclamation by thermal decomposition only was also conducted. In Fig. 4a, the integrity rate of Si-wafers using the SSTD process (86.11%) is nearly

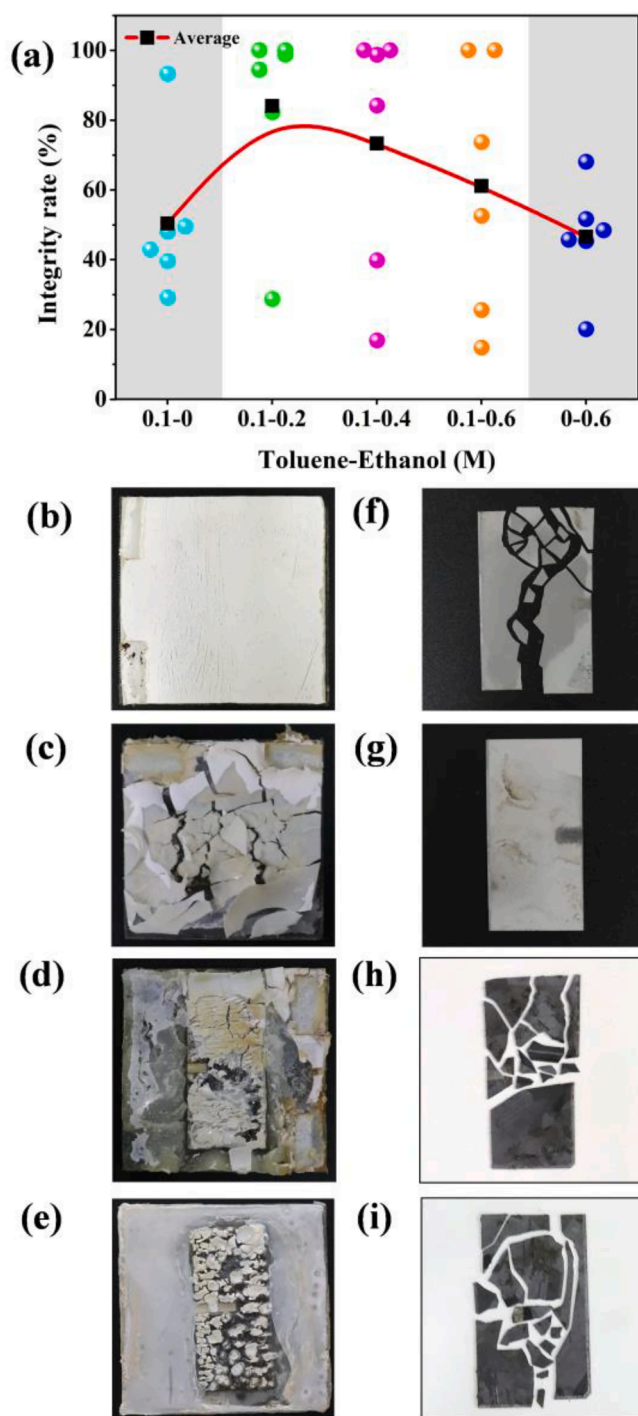


Fig. 3. (a) Variation of the integrity rate with ethanol addition and back pictures of modules treated with a mixed solvent of toluene-ethanol with ratios of (b) 0.1–0 M, (c) 0.1–0.2 M, (d) 0.1–0.6 M, and (e) 0–0.6 M, and pictures for reclaimed cells pretreated with (f) 0.1–0 M, (g) 0.1–0.2 M, (h) 0.1–0.6 M and (i) 0–0.6 M toluene-ethanol.

10-fold higher than that of thermal decomposition alone (9.26%). Such high integrity rate in the scale-up facility demonstrates the satisfying feasibility and easy scaling up feature of the proposed novel SSTD technology.

Moreover, the consumption of organic solvents during scale-up verification was analyzed by GC–MS. As shown in Fig. 4b, the relative contents of toluene and ethanol in the mixed organic solvents present a negligible decrease after three recycles. In solvothermal treatment

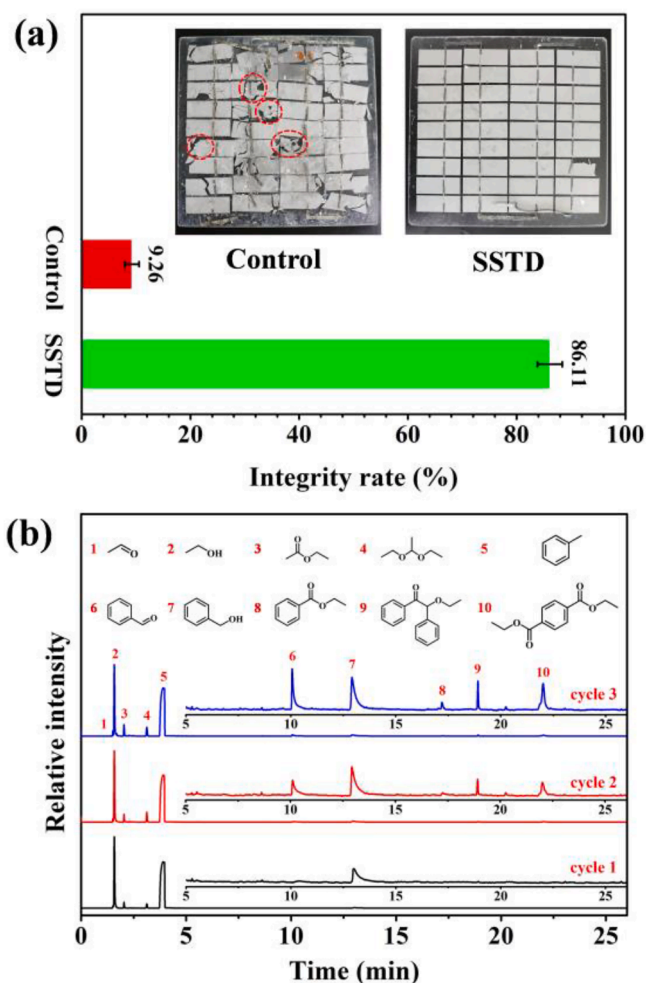


Fig. 4. (a) Integrity rate of wafers reclaimed from commercial modules and (b) organic solvent consumption during scale-up verification.

process, ethanol is consumed as a reactant in the chemical degradation of backsheets, and toluene takes part in the swelling of EVA. Fortunately, both backsheets and EVA account for low proportions of PV modules, with proportions of 1.91% and 4.52% by weight, respectively [32]. Therefore, the low consumption of organic solvents is reasonable, and the result can illustrate the environmental friendliness of this recovery system.

The superiority of the SSTD process over other technologies is highlighted by comparing the operating conditions and Si-wafer integrity rates. As shown in Table 1, the SSTD process clearly outperforms most of the previous technologies for Si-wafers recovery from PV modules. Immersing PV modules in trichloroethylene at 80 °C for 7–10 days was used to successfully recover cells without any damage [16]. However, mechanical pressure must be adjusted to modules, and a long operating time is always necessary, which is difficult in practical applications. In addition, the thickness is a crucial factor affecting the recycling difficulty and integrity rate of Si-wafers. The thicker the cells are, the higher the integrity rate and the lower recycling difficulty. It is reasonably speculated that the thickness of Si-cells used in studies before 2006 [16] is much higher than that of the Si-cells used in this study. Thus, the high integrity rate of thinner Si-wafer recovered from PV modules makes the SSTD process more instructive, and it has practical application prospects [25]. In addition, the originality of the research lies in the first application of hot organic solvents vapor, rather than immersion in organic solvents to achieve EVA swelling, exhibiting significant time saving. Other efficient technologies were also designed to recover unbroken cells in a short operating time. Park et al. [28]

**Table 1**  
PV module separation and recycling technologies.

Technology	Condition	Module type	Operating time	Integrity	Ref.
Inorganic acid dissolution	HNO <sub>3</sub>	c-Si	25 h	Broken	[15]
Solvent dissolution	Trichloroethylene (80 °C) with mechanical pressure	One-cell c-Si	7–10 d	Unbroken	[16]
Solvent dissolution	Toluene (70 °C, ultrasonic irradiation-900 W)	One-cell c-Si	1 h	Broken	[31]
Solvent dissolution	Physical process-Toluene (60 °C, ultrasonic-200 W)	Commercial c-Si fragment	2 h	Broken	[33]
Thermal decomposition	600 °C (12.8 °C·min <sup>-1</sup> )	Commercial c-Si fragment	30 min	Broken	[18]
Thermal decomposition	500 °C after mechanically backsheet removal	Commercial c-Si	1 h	Broken	[19]
Thermal decomposition	480 °C (15 °C·min <sup>-1</sup> ) with a fixture	One-cell c-Si	30 min	Unbroken	[28]
Thermal decomposition	520 °C after glass cracking and EVA patterning	One-cell c-Si	30 min	Unbroken	[29]
Thermal decomposition	500 °C	Commercial c-Si fragment	30 min	Broken	[34]
Solvent dissolution-thermal decomposition	Toluene (90 °C)-thermal decomposition (600 °C)	Commercial c-Si	49 h	Broken	[17]
High voltage fragmentation	160 kV	Commercial c-Si fragment	/	Broken	[35]
SSTD process	Solvothermal swelling (190 °C)-thermal decomposition (500 °C)	One-cell and commercial c-Si	2 h	Unbroken	This work

employed a fixture to force decomposition gas to release in the horizontal direction. However, this process required rigorous conditions of a specific heating rate (15 °C·min<sup>-1</sup>) and proper pressure loading. As it is better to divert rather than block, Lee et al. [29] built gas release paths by cracking glass and patterning EVA. This method worked but was not stable because tempered glass has compressive stress, which may lead to uncontrollable glass cracking and premature Si-cell breakage. In contrast, the SSTD process brings forward a novel stable and promising method for practical application. Compared to thermal treatment directly, solvothermal swelling provides milder condition that EVA decomposition gas release channels can be created without any other fixture or cracking. In this regard, not only the Si-cell, but also tempered glass could be reclaimed without any damage.

To the best of our knowledge, all the technologies ever reported to

recover unbroken wafers tend to choose mini-modules (one-cell modules) as experimental samples. In this work, the mini-modules are only used in the operating parameter optimization, while the scale-up demonstration changes to the use of commercial modules, indicating the greater persuasiveness of our results. Another interesting note is the specially designed solvents used in solvothermal swelling process. Different from all other existing methods, ethanol is introduced in this work to removal backsheet in advance. As a result, the gaseous exhausts containing fluorinated compounds derived from backsheet burning in the following thermal decomposition would be avoided.

### 3.3. Process mechanism

The process mechanism of efficient nondestructive Si-wafer recovery

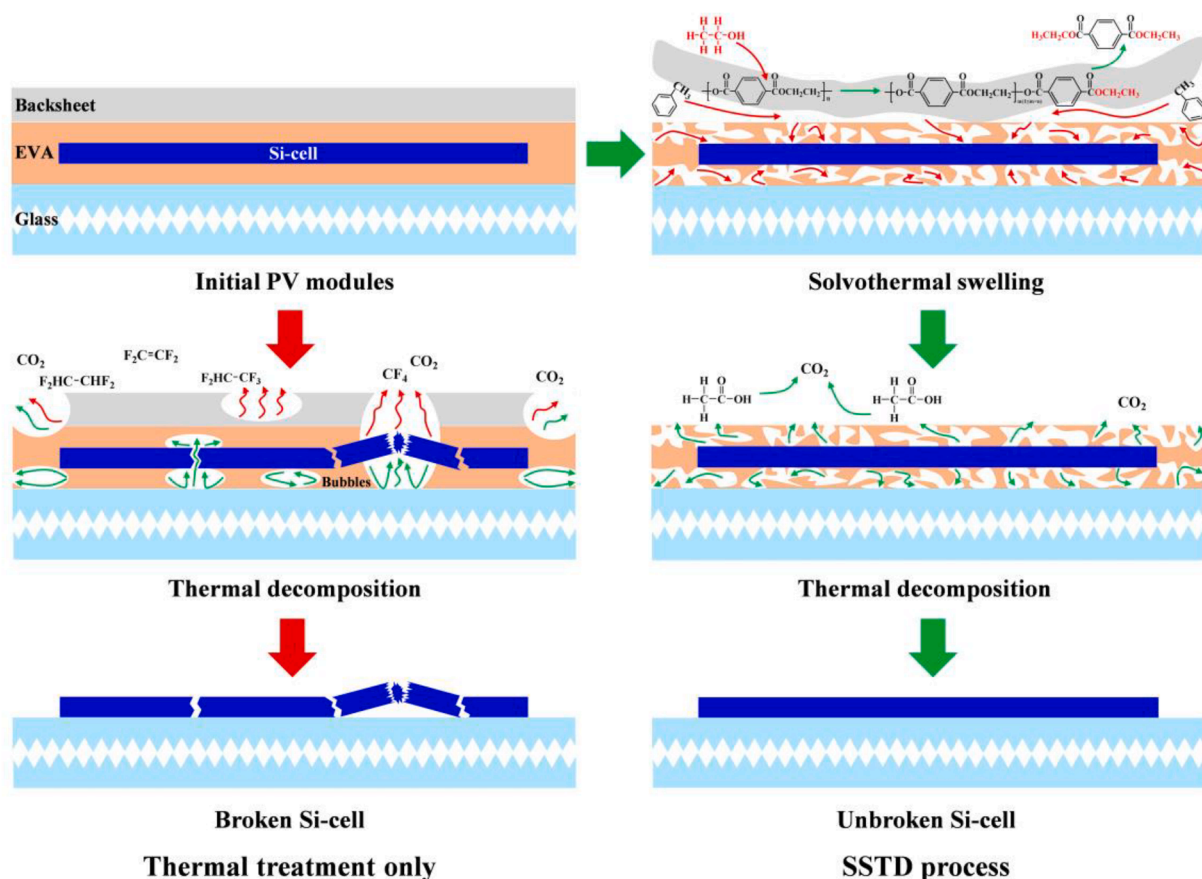


**Fig. 5.** Process mechanism for Si-cell recovery from modules by only thermal decomposition (red path) and the SSTD process (green path).

by the SSTD process is proposed, as shown in Fig. 5. The key of the SSTD process is to swell EVA to build gas release channels, delivering Si-wafer from EVA decomposition gas stress. Therefore, the mechanism of solvothermal swelling was the focus of this study. Owing to the introduction of ethanol, depolymerization of the backsheets occurred firstly in solvothermal swelling process. By GC-MS analysis (Fig. S3), besides the oxides of toluene (benzaldehyde and benzyl alcohol) and reaction products of ethanol and its oxides (ethyl acetate, 1,1-diethoxyethane, etc.), the major component is diethyl terephthalate which is considered as the degradation product of PET glycolysis. Then, the Tedlar/PET/Tedlar sandwich structure of the backsheets is destroyed and the backsheets removal is consequently obtained due to the PET glycolysis. In fact, glycolysis with alcohols has been proven to be an efficient method for PET degradation and recovery. Under the condition of 190 °C, ethanol in solvothermal swelling system could reach subcritical state, which has been proved to be effective for PET glycolysis even without metal catalysts [36,37]. In the process, the carbonyl oxygen of PET is susceptible to attack, and therefore carbonyl carbon with a more partial positive charge is achieved. In this regard, a pair of unshared electrons on the hydroxyl oxygen of ethanol attacks the carbonyl carbon of PET, creating a new carbon-oxygen bond between ethanol and PET. At the same time, carbon-oxygen bond of PET is broken, contributing to polymer chain breakage and PET depolymerization [38]. With adequate ethanol, PET is depolymerized to monomer diethyl terephthalate, which destroys the sandwich structure, leading to the removal of backsheets. In this way, the contact area between EVA and toluene was extremely enlarged, accelerating the EVA swelling process. As depicted in Fig. S3, no EVA-related degradation products or monomers were observed in organic solvents after solvothermal swelling. In this case, it can be speculated that diffusing macromolecules into organic solvents is the main transformation of EVA. EVA is a typical polymer, whose dissolution involves two processes: solvent diffusion and chain disentanglement. Compared to the polymer EVA, toluene presents an excellent diffusion rate. Therefore, the macroscopic volume of EVA is firstly expanded as toluene molecules diffuse into the polymer network. Then, the macromolecular segment motion is enhanced and toluene molecules effectively break polymer chains, leading to the EVA separation [39]. However, the above process takes long time of weeks at a lower temperature and pressure. By optimizing the operating parameters of solvothermal swelling, the process is accelerated greatly under the condition of 190 °C, 2 h processing duration, 0.2 M toluene and 0.2 M

ethanol, contributing to the gas release channels formation.

In the following thermal treatment process, the residual EVA is removed completely. According to the thermogravimetric analysis, EVA thermal decomposition can be divided into two major stages in an air ambient. The first stage (300–400 °C) is the vinyl acetate groups removal, which is designated as a deacetylation process; the residue main chain is decomposed completely into carbon oxides in the second stage, at 420–450 °C [19,40]. By thermal decomposition alone, the Si-wafers breakage begins to occur in the first stage, in which a large amount of gas is releasing, and aggravates in the following stage. In SSTD process, the decomposition gas escapes along the release channels built in advance, and thus nondestructive Si-cells are reclaimed.

### 3.4. Characteristics of reclaimed wafers

To be reused for the manufacturing of new PV module, the characteristics of reclaimed nondestructive Si-wafers are of significant importance. The surface impurities, including metal electrodes and antireflective coating ( $\text{SiN}_x$ ) on Si-cells are removed by chemical etching to obtain Si-wafers. The surface chemical compositions of the new cell, reclaimed cell and reclaimed wafer were analyzed by EDS. As presented in Figs. 6 and S4, the oxygen (O), silver (Ag) and aluminum (Al) in front and back metal electrodes are successfully removed. In addition, the disappearance of nitrogen (N) indicates the removal of antireflective coating, which could be further proved by the XPS analysis (Fig. 7a).

After cleaning and purifying of the reclaimed cell by chemical etching, the significant and basic properties of pure reclaimed wafers, including interstitial oxygen, substitutional carbon, resistivity and minority carrier lifetime, were measured according to the GB/T 29054-2019 standard for raw pure Si-wafers. A proper amount of interstitial oxygen enhances the mechanical property and adsorbs metals in silicon as intrinsic gettering. In contrast, excess interstitial oxygen could dramatically lead to warpage and damage of Si-wafers [41]. In addition, high substitutional carbon is believed to be detrimental to the potential risk of increasing the leakage current [42]. Therefore, the interstitial oxygen and substitutional carbon must be controlled below the limits of  $6 \times 10^{17}$  and  $5 \times 10^{17}$  atoms·cm<sup>-3</sup>, respectively, according to the Chinese National Standard of GB/T 29054-2019. As presented in Fig. 7b, the concentrations of O and C in the reclaimed wafers are both lower than the above limit value, demonstrating that interstitial oxygen and substitutional carbon certainly meet the requirements. This is to be

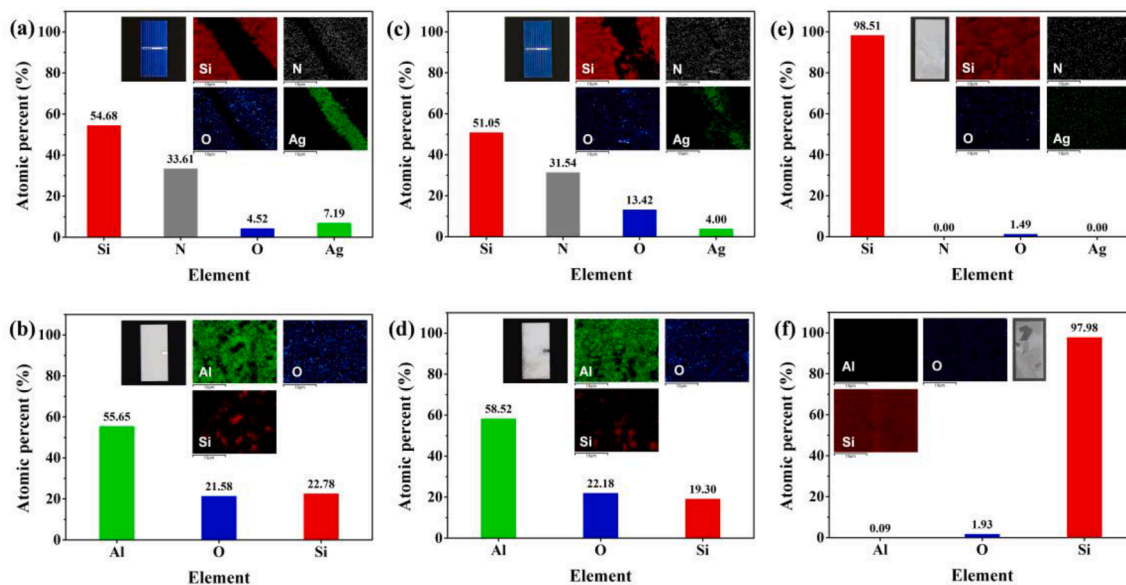
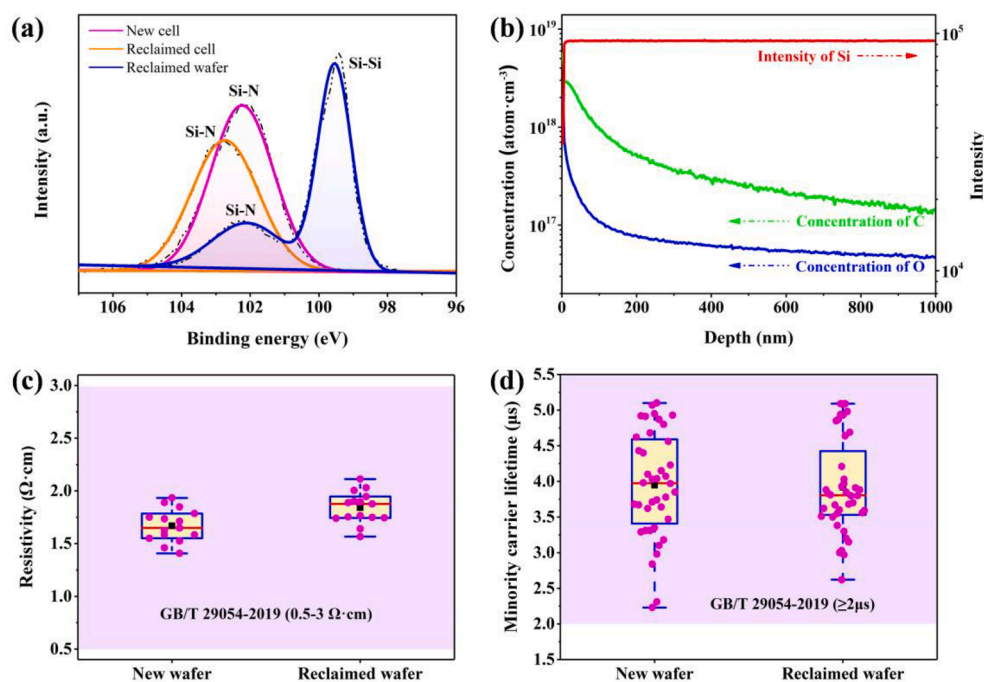


Fig. 6. EDS analysis and mapping images of the (a) front and (b) back surfaces of the new cell, (c) front and (d) back surfaces of the reclaimed cell, and (e) front and (f) back surfaces of the reclaimed wafer.



**Fig. 7.** (a) Si 2p XPS spectra of new cell, reclaimed cell and reclaimed wafer, (b) SIMS spectra of the O and C contents in the reclaimed wafers, (c) resistivity measurements of new wafers and reclaimed wafers and (d) minority carrier lifetimes of new wafers and reclaimed wafers.

expected that the Si-wafers are reclaimed without any damage by SSTD process to avoid the silicon ingot production process, in which interstitial oxygen and substitutional carbon are inevitable impurities.

As one of the basic properties of a semiconducting material, the resistivity is directly related to the doping concentration. For Si-cells, the resistivity is commonly used to characterize the effects of doping, metal deposition and resistive paste printing [43]. Generally, a lower doping concentration increases the resistivity and enhances the short-circuit current, while a higher doping concentration decreases the resistivity and enhances the open circuit voltage [44]. Therefore, an appropriate resistivity is required to achieve the high efficiency of PV modules, which is specified between 0.5 and 3.0 Ω·cm (GB/T 29054-2019). In Fig. 7c, there is no significant difference in resistivity between new wafers and reclaimed wafers, and both lie in the range of 1.0–2.5 Ω·cm, with average resistivity of 1.67 and 1.84 Ω·cm, respectively. This indicates that the doping concentration changes little and that no other negative effects on the resistivity are introduced by the SSTD process. The resistivity of reclaimed wafers is acceptable according to the guidelines for new PV module fabrication.

The minority carrier lifetime, the time it takes the minority carrier concentration to decrease to 1/e of the original value, is another critical parameter to determine the cell efficiency. The crystallographic imperfections and impurities in Si-wafers have a vital impact on the minority carrier lifetime [45]. A higher minority carrier lifetime represents higher cell efficiency. Accordingly, extra crystallographic imperfections and impurities should be avoided during the recovery process. As shown in Fig. 7d, the average minority carrier lifetime of the reclaimed wafers is 3.92 μs and falls in the GB/T 29054-2019 standard value range (≥2 μs), which is similar to the values of new wafers (3.95 μs). This result suggests that the crystallographic imperfections and impurities introduced by the SSTD process are negligible. All the properties of reclaimed wafers are quite similar to those of original new wafers, which directly proves the reusability of reclaimed wafers. In short, the developed novel SSTD process shows promising prospects for nondestructive Si-wafer recycling from PV waste.

#### 4. Conclusion

In this work, a novel process that integrates solvothermal swelling and thermal decomposition for nondestructive Si-wafer recovery from PV modules is developed. Under the optimized laboratory-scale condition (190 °C, 2 h and 0.2 M toluene), structure-intact Si-wafers are reclaimed. An average integrity rate of 86.11%, which is nearly 10-fold higher than that of thermal decomposition alone (9.26%), is obtained using a scaling up facility. After chemical etching, the interstitial oxygen ( $<6 \times 10^{17}$  atoms·cm<sup>-3</sup>), substitutional carbon ( $<5 \times 10^{17}$  atoms·cm<sup>-3</sup>), resistivity (~1.84 Ω·cm) and minority carrier lifetime (~3.92 μs) of reclaimed wafers are tested and proven to be satisfactory for the manufacturing of new PV module. The key to the successful recovery of nondestructive Si-wafers is to realize the quick release of EVA decomposition gas in the horizontal direction during thermal decomposition through the preformed gas release channels by swelling EVA in advance. The EVA swelling method of exposing PV modules in hot and pressurized organic vapors, rather than immersing in solvent, is firstly applied for nondestructive Si-wafers recovery, which presents significant superiority in time and solvents saving as well as a high recycling integrity rate to previous technologies. In addition, the introduction of ethanol is original and efficient to remove PV backsheets to accelerate EVA swelling and avoid the fluorine-containing gases emission, suggesting a more environmental-friendly feature of the SSTD process. Therefore, the SSTD process has been demonstrated as a feasible method for massive nondestructive Si-wafer recovery and EoL PV waste treatment.

#### Declaration of Competing Interest

The authors declare that they have no known competing financial interests or personal relationships that could have appeared to influence the work reported in this paper.

#### Acknowledgements

This work is supported by the “Strategic Priority Research Program (A)” of the Chinese Academy of Sciences (XDA23030301), the

FJIRSM&IUE Joint Research Fund (RHZX-2018-001), the Industry Leading Key Projects of Fujian Province (2019H0056) and the Science and Technology Program of Xiamen (3502Z20203074).

## Appendix A. Supplementary data

Supplementary data to this article can be found online at <https://doi.org/10.1016/j.cej.2021.129457>.

## References

- [1] IEA Installed power generation capacity in the Stated Policies Scenario, 2000–2040, <https://www.iea.org/data-and-statistics/charts/installed-power-generation-capacity-in-the-stated-policies-scenario-2000-2040>.
- [2] F. Corcelli, M. Ripa, S. Ulgiati, End-of-life treatment of crystalline silicon photovoltaic panels. An emergy-based case study, *J. Cleaner Prod.* 161 (2017) 1129–1142.
- [3] R. Deng, N.L. Chang, Z. Ouyang, C.M. Chong, A techno-economic review of silicon photovoltaic module recycling, *Renew. Sustain. Energy Rev.* 109 (2019) 532–550.
- [4] B. Jung, J. Park, D. Seo, N. Park, Sustainable system for raw-metal recovery from crystalline silicon solar panels: from noble-metal extraction to lead removal, *ACS Sustainable Chem. Eng.* 4 (2016) 4079–4083.
- [5] H. He, Y. Gutierrez, T.M. Young, J.M. Schoenung, The role of data source selection in chemical hazard assessment: a case study on organic photovoltaics, *J. Hazard. Mater.* 365 (2019) 227–236.
- [6] P. Nain, A. Kumar, Ecological and human health risk assessment of metals leached from end-of-life solar photovoltaics, *Environ. Pollut.* 267 (2020), 115393.
- [7] M. Tammaro, A. Salluzzo, J. Rimauro, S. Schiavo, S. Manzo, Experimental investigation to evaluate the potential environmental hazards of photovoltaic panels, *J. Hazard. Mater.* 306 (2016) 395–405.
- [8] T. Zhang, Z. Dong, F. Qu, F. Ding, X. Peng, H. Wang, H. Gu, Removal of CdTe in acidic media by magnetic ion-exchange resin: a potential recycling methodology for cadmium telluride photovoltaic waste, *J. Hazard. Mater.* 279 (2014) 597–604.
- [9] Y.S. Zimmermann, A. Schaeffer, F.X. Corvini, M. Lenz, Thin-film photovoltaic cells: long-term metal(loid) leaching at their end-of-life, *Environ. Sci. Technol.* 47 (2013) 13151–13159.
- [10] I. Celik, B.E. Mason, A.B. Phillips, M.J. Heben, D. Apul, Environmental impacts from photovoltaic solar cells made with single walled carbon nanotubes, *Environ. Sci. Technol.* 51 (2017) 4722–4732.
- [11] M.L. Bustamante, G. Gaustad, Challenges in assessment of clean energy supply-chains based on byproduct minerals: a case study of tellurium use in thin film photovoltaics, *Appl. Energy* 123 (2014) 397–414, <https://doi.org/10.1016/j.apenergy.2014.01.065>.
- [12] A.J. Hunt, A.S. Matharu, A.H. King, J.H. Clark, The importance of elemental sustainability and critical element recovery, *Green Chem.* 17 (2015) 1949–1950.
- [13] F.C.S.M. Padoan, P. Altimari, F. Pagnanelli, Recycling of end of life photovoltaic panels: a chemical prospective on process development, *Sol. Energy* 177 (2019) 746–761, <https://doi.org/10.1016/j.solener.2018.12.003>.
- [14] Y.S. Zimmermann, C. Niewersch, M. Lenz, Z.Z. Kül, F.X. Corvini, A. Schäffer, T. Wintgens, Recycling of indium from CIGS photovoltaic cells: potential of combining acid-resistant nanofiltration with liquid-liquid extraction, *Environ. Sci. Technol.* 48 (2014) 13412–13418.
- [15] T.M. Bruton, Re-cycling of high value, high energy content components of silicon PV modules, in: *Proceedings of the 12th EC-PVSEC, 1994*, pp. 303–304.
- [16] T. Doi, I. Tsuda, H. Unagida, A. Murata, K. Sakuta, K. Kurokawa, Experimental study on PV module recycling with organic solvent method, *Sol. Energy Mater. Sol. Cells* 67 (1–4) (2001) 397–403, [https://doi.org/10.1016/S0927-0248\(00\)00308-1](https://doi.org/10.1016/S0927-0248(00)00308-1).
- [17] S. Kang, S. Yoo, J. Lee, B. Boo, H. Ryu, Experimental investigations for recycling of silicon and glass from waste photovoltaic modules, *Renewable Energy* 47 (2012) 152–159, <https://doi.org/10.1016/j.renene.2012.04.030>.
- [18] M. Tammaro, J. Rimauro, V. Fiandra, A. Salluzzo, Thermal treatment of waste photovoltaic module for recovery and recycling: experimental assessment of the presence of metals in the gas emissions and in the ashes, *Renewable Energy* 81 (2015) 103–112, <https://doi.org/10.1016/j.renene.2015.03.014>.
- [19] V. Fiandra, L. Sannino, C. Andreozzi, F. Corcelli, G. Graditi, Silicon photovoltaic modules at end-of-life: removal of polymeric layers and separation of materials, *Waste Manage.* 87 (2019) 97–107.
- [20] J. Shin, J. Park, N. Park, A method to recycle silicon wafer from end-of-life photovoltaic module and solar panels by using recycled silicon wafers, *Sol. Energy Mater. Sol. Cells* 162 (2017) 1–6, <https://doi.org/10.1016/j.solmat.2016.12.038>.
- [21] V. Aryan, M. Font-Brucart, D. Maga, A comparative life cycle assessment of end-of-life treatment pathways for photovoltaic backsheets, *Prog. Photovolt. Res. Appl.* 26 (2017) 443–459.
- [22] V. Fiandra, L. Sannino, C. Andreozzi, G. Graditi, End-of-life of silicon PV panels: a sustainable materials recovery process, *Waste Manage.* 84 (2018) 91–101.
- [23] L. Zhang, Z. Xu, Separating and recycling plastic, glass, and gallium from waste solar cell modules by nitrogen pyrolysis and vacuum decomposition, *Environ. Sci. Technol.* 50 (2016) 9242–9250.
- [24] W.-H. Huang, W.J. Shin, L. Wang, W.-C. Sun, M. Tao, Strategy and technology to recycle wafer-silicon solar modules, *Sol. Energy* 144 (2017) 22–31, <https://doi.org/10.1016/j.solener.2017.01.001>.
- [25] ISE, Photovoltaics Report, <https://www.ise.fraunhofer.de/content/dam/ise/de/documents/publications/studies/Photovoltaics-Report.pdf>.
- [26] J. Li, Y. Lin, F. Wang, J. Shi, J. Sun, B. Ban, G. Liu, J. Chen, Progress in recovery and recycling of kerf loss silicon waste in photovoltaic industry, *Sep. Purif. Technol.* 254 (2021), 117581.
- [27] J. Kong, Y. Zhuang, P. Xing, H. Yin, X. Luo, Recycling high purity silicon from solar grade silicon cutting slurry waste by carbothermic reduction in the electric arc furnace, *J. Cleaner Prod.* 224 (2019) 709–718.
- [28] J. Park, W. Kim, N. Cho, H. Lee, N. Park, An eco-friendly method for reclaimed silicon wafers from a photovoltaic module: from separation to cell fabrication, *Green Chem.* 18 (2016) 1706–1714.
- [29] J.-K. Lee, J.-S. Lee, Y.-S. Ahn, G.-H. Kang, H.-E. Song, M.-G. Kang, Y.-H. Kim, C.-H. Cho, Simple pretreatment processes for successful reclamation and remanufacturing of crystalline silicon solar cells, *Prog. Photovolt. Res. Appl.* 26 (3) (2018) 179–187, <https://doi.org/10.1002/pip.2963>.
- [30] D. Prat, A. Wells, J. Hayler, H. Sneddon, C.R. McElroy, S. Abou-Shehata, P.J. Dunn, CHEM21 selection guide of classical- and less classical-solvents, *Green Chem.* 18 (1) (2016) 288–296, <https://doi.org/10.1039/C5GC01008J>.
- [31] Y. Kim, J. Lee, Dissolution of ethylene vinyl acetate in crystalline silicon PV modules using ultrasonic irradiation and organic solvent, *Sol. Energy Mater. Sol. Cells* 98 (2012) 317–322, <https://doi.org/10.1016/j.solmat.2011.11.022>.
- [32] J.R. Duflo, J.R. Peeters, D. Altamirano, E. Bracquene, W. Dewulf, Demanufacturing photovoltaic panels: comparison of end-of-life treatment strategies for improved resource recovery, *CIRP Ann.* 67 (1) (2018) 29–32, <https://doi.org/10.1016/j.cirp.2018.04.053>.
- [33] M.F. Azeumo, C. Germana, N.M. Ippolito, M. Franco, P. Luigi, S. Settimo, Photovoltaic module recycling, a physical and a chemical recovery process, *Sol. Energy Mater. Sol. Cells* 193 (2019) 314–319, <https://doi.org/10.1016/j.solmat.2019.01.035>.
- [34] P. Dias, S. Javimczik, M. Benevit, H. Veit, Recycling WEEE: polymer characterization and pyrolysis study for waste of crystalline silicon photovoltaic modules, *Waste Manage.* 60 (2016) 716–722.
- [35] B.P. Song, M.Y. Zhang, Y. Fan, L. Jiang, J. Kang, T.T. Gou, C.L. Zhang, N. Yang, G. J. Zhang, X. Zhou, Recycling experimental investigation on end of life photovoltaic panels by application of high voltage fragmentation, *Waste Manage.* 101 (2020) 180–187.
- [36] M. Imran, B.K. Kim, M. Han, B.G. Cho, D.H. Kim, Sub- and supercritical glycolysis of polyethylene terephthalate (PET) into the monomer bis(2-hydroxyethyl) terephthalate (BHET), *Polym. Degrad. Stabil.* 95 (2010) 1686–1693.
- [37] Q. Wang, X. Yao, S. Tang, X. Lu, X. Zhang, S. Zhang, Urea as an efficient and reusable catalyst for the glycolysis of poly(ethylene terephthalate) wastes and the role of hydrogen bond in this process, *Green Chem.* 14 (2012) 2559–2566.
- [38] A.M. Al-Sabagh, F.Z. Yehia, D. Harding, G. Eshaq, A.E. Elmetwally, Fe<sub>3</sub>O<sub>4</sub>-boosted MWCNT as an efficient sustainable catalyst for PET glycolysis, *Green Chem.* 18 (2016) 3997–4003.
- [39] Y.W. Fan, K.X. Liu, L.L. Zhang, H. Zhao, J.F. Chen, Rapid and continuous polymer dissolution by rotating packed bed for enhanced oil recovery, *Chem. Eng. Process.* 153 (2020), 107952.
- [40] A. Badiie, I.A. Ashcroft, R.D. Wildman, The thermo-mechanical degradation of ethylene vinyl acetate used as a solar panel adhesive and encapsulant, *Int. J. Adhes. Adhes.* 68 (2016) 212–218.
- [41] J. Zhao, P. Dong, J.J. Zhao, X.Y. Ma, D.R. Yang, Impact of germanium co-doping on oxygen precipitation in heavily boron-doped Czochralski silicon, *Superlattice Microstruct.* 99 (2016) 35–40.
- [42] Y. Sun, T. Zhao, W. Lan, J. Zhao, Z. Ni, J. Zhao, X. Yu, X. Ma, D. Yang, Revisiting the effects of carbon-doping at 10<sup>17</sup> cm<sup>-3</sup> level on dislocation behavior of Czochralski silicon: from room temperature to elevated temperatures, *J. Membr. Sci.* 30 (2019) 3114–3123.
- [43] A. Richter, J. Benick, F. Feldmann, A. Fell, M. Hermlé, S.W. Glunz, n-Type Si solar cells with passivating electron contact: identifying sources for efficiency limitations by wafer thickness and resistivity variation, *Sol. Energy Mater. Sol. Cells* 173 (2017) 96–105, <https://doi.org/10.1016/j.solmat.2017.05.042>.
- [44] M.D. Johnston, M. Barati, Distribution of impurity elements in slag-silicon equilibria for oxidative refining of metallurgical silicon for solar cell applications, *Sol. Energy Mater. Sol. Cells* 94 (12) (2010) 2085–2090, <https://doi.org/10.1016/j.solmat.2010.06.025>.
- [45] J. John, A. Hajjiah, M. Haslinger, M. Soha, A. Uruena, E. Cornagliotti, L. Tous, P. Mertens, J. Poortmans, Deposition behaviour of metal impurities in acidic cleaning solutions and their impact on effective minority carrier lifetime in n-type silicon solar cells, *Sol. Energy Mater. Sol. Cells* 194 (2019) 83–88, <https://doi.org/10.1016/j.solmat.2019.02.001>.